8-13-2021

Substrate temperature effects on the peel behavior of temporary pavement marking tapes

Hyeyoung Son

Kendra Erk

Chelsea Davis

The Journal of Adhesion

Hyeyoung Son[a], Kendra A. Erk[a], Chelsea S. Davis[a*]

[a]*School of Materials Engineering, Purdue University, West Lafayette, United States;*

Hyeyoung Son

School of Materials Engineering

Purdue University, West Lafayette, IN, USA, 47907

Email: son49@purdue.edu

Kendra A. Erk

School of Materials Engineering

Purdue University, West Lafayette, IN, USA, 47907

Email: erk@purdue.edu

ORCiD: 0000-0001-9238-1928

Chelsea S. Davis

School of Materials Engineering

Purdue University, West Lafayette, IN, USA, 47907

Email: chelsea@purdue.edu (*Corresponding Author)

ORCiD: /0000-0002-0383-7717

Substrate temperature effects on the peel behavior of temporary pavement marking tapes

Temporary pavement marking (TPM) tapes are utilized in road construction to delineate temporary traffic lanes and work zones. Adhesive failure of TPM tapes can therefore remove lane and work zone designations, confusing drivers and causing serious accidents, especially in high speed zones. Thus, the adhesion of TPM tapes to pavement surface plays an important role in road construction traffic safety. Pressure sensitive adhesives (PSAs) comprise the adhesive layer of TPM tapes. The adhesion of PSAs depends on their temperature-dependent viscoelastic properties. Since environmental conditions vary during construction, the adhesion of TPM tapes will change over a range of operating temperatures. The viscoelastic properties and peel force of four brands of commercial TPM tapes were characterized via double lap shear dynamic mechanical analysis and 90° angle peel adhesion testing over a range of temperatures (-20 °C to 40 °C). The interfacial fracture behavior and peel forces were analyzed with respect to the measured viscoelastic properties of TPM tapes. For temperatures below the glass transition temperature of the top layer and the transition temperature into the rubbery plateau of the PSA, the peel force decreased. Through this simple technique, an effective operating temperature range for each TPM tape was determined.

Keywords: Temporary pavement marking tape, Pressure sensitive, viscoelasticity, peel, dynamic mechanical analysis

1. Introduction

Temporary pavement marking (TPM) tape plays an important role on the roadway during construction – it designates temporary traffic lanes and construction work zones. TPM tapes must be visible, durable, and easily removed to prevent damaging the roadway and ensure driver's safety. [1–3] Thus, the precise adhesion of TPM tapes to pavements is a primary concern since too weak adhesion causes dangerous premature adhesive failure and too strong adhesion damages the roadway surface upon removal, leaving residual markings or "ghost marks".[4] Even though the adhesion of TPM tapes is essential to their performance, there is no governing industrial standard for the adhesion of TPM tapes. Therefore, it is necessary to understand the effect of materials properties on the adhesion of TPM tapes to establish these industrial standards. Figure 1 shows the typical structure of TPM tapes, which consist of an elastomeric top layer, fiber/fabric reinforcing layer, and a pressure sensitive adhesive (PSA) layer. The PSA and reinforcing fabrics are located on the bottom surface of the TPM tape. Since each TPM tape is comprised of various polymers, it is not surprising that the mechanical properties, as well as bond strength, vary with temperature.[5–8] Even though road construction is typically conducted during the warmer part of the year, it is necessary to evaluate the performance of TPM tapes in various environments as average temperatures and weather conditions vary diurnally and from day to day.

[Figure 1 near here]

PSA is the most widely used non-structural adhesive in applications such as packaging, architecture, and medicine.[9] PSAs govern the adhesion of TPM tapes, and as such it is important to understand their mechanical properties. Many previous studies show that the performance of a PSA is strongly dependent on the PSA's bulk viscoelastic properties.[10–18] The elastic modulus or shear modulus affects conformability to rough surfaces and the viscous component is linked with

energy dissipation upon debonding.[19] The viscoelastic properties of PSA's are highly dependent on temperature. Thus, temperature variability must be considered for PSAs used in outdoor construction applications, such as on roadways in work zones.[6,20]

The dynamic mechanical properties of PSAs can be divided into four different zones as a function of increasing temperature: a glassy zone, glass transition zone, rubbery plateau zone, and terminal zone.[6] At the lowest temperatures, in the glassy zone, a PSA is a glassy elastic material, characterized by a high modulus. As the temperature increases, in the glass transition zone, the modulus of a PSA sharply decreases, and it becomes flexible. In the rubbery plateau zone, a PSA is viscoelastic and has constant storage and loss moduli. Finally, at the highest temperatures, in the terminal zone, the PSA has a low modulus and is viscous, tending to flow. The debonding behavior of a PSA changes depending on these viscoelastic properties.[16,21] In the terminal zone, PSAs fail cohesively during peeling, while in the rubbery plateau zone they adhesively fail. [21] In the glass transition and glassy zones, a PSA fails by brittle interfacial fracture.[16]

In this study, 90° peel tests were performed on substrates held at constant temperatures, ranging from -20 °C to 40 °C, to evaluate the temperature dependence of PSA adhesion. The viscoelastic properties of PSAs and top layers of four brands of TPM tape were measured within potential operating temperatures which simulate the use of TPM tapes in typical as well as extreme construction conditions. By analyzing the peeling behavior and the viscoelastic properties, ideal operating temperatures were identified for each TPM tape.

2. Materials and Methods

[Figure 2 near here]

2.1 Materials

Four different commercially available TPM tapes, labeled A, B, C, and D, were tested. Figure 1 (b) and (c) show the top and cross-section views of each tape, respectively. Tapes A and C have ridges on the top layer surface, while Tape B and D do not. Each tape has a unique composition resulting in different mechanical properties and geometries. The thicknesses of the PSA and top layer were measured with an optical microscope (DMi8, Leica). A summary of these sizes is reported in Table 1.

[Table 1 near here]

2.2 Dynamic mechanical analysis of PSA and top layer of TPM tapes

The dynamic mechanical properties of PSAs were measured in a double lap shear geometry. Figure 2 (a) shows the custom-built double lap shear fixture used to measure the dynamic mechanical properties of the PSA. Tapes were cut into 12mm by 8mm specimens and the PSA side was attached to both sides of the center portion of the fixture as shown in the inset of Figure 2(a). The top layer was fixed to the outer supports of the fixture with ethyl cyanoacrylate glue (Loctite, Henkel). The double lap shear fixture was assembled with screws. In order to apply shear to the TPM tapes' PSA layers, these rigid supports were clamped to the tensile oscillator of the dynamic mechanical analysis (DMA, Q850, TA Instrument) instrument. Subsequently, a simple uniaxial tensile configuration of the DMA was used to measure the dynamic mechanical properties of the top layer of each TPM. These DMA tensile samples were prepared by cutting 12mm by 30mm specimens after carefully removing the PSA and reinforcing fabrics.

The dynamic mechanical properties of both the PSA and top layer on TPM tapes were measured using an oscillatory strain with a linear temperature sweep function through DMA. A 0.5% oscillatory shear strain was applied to the PSA of each tape with the double lap shear fixture at a frequency of 1 Hz. A 0.2% oscillatory tensile strain was applied to the top layer samples at a

frequency of 1 Hz. The temperature was increased from -20 °C to 40 °C in 5 °C increments, and the dwell time was 120s at each temperature.

2.3 Peel Test

90° angle peel adhesion testing was chosen to evaluate the peel force of TPM tapes since it is a straightforward and commonly used technique to directly quantify the adhesion of tapes. 90° peel tests were performed with a custom-built modular peel fixture. TPM tape peel tests were conducted on substrates held at -20 °C, 0 °C, 25 °C, and 40 °C, as shown in Figure 2 (b). The peel fixture has been fully described in previous work.[25] A stainless-steel substrate was used for all tests since it has good thermal conductivity, allowingto the set temperature to be achieved quickly and maintained over the course of eachpeel test. A thermocouple was placed on the substrate near the peel specimen to monitor the substrate temperature during each peel test. To achieve the desired temperatures, a stainless-steel container was placed directly under the substrate and was filled with dry ice or ice with table salt to attain substrate temperatures of -20 °C or 0 °C, respectively. For measurements at 25 °C and 40 °C, the stainless-steel substrate was placed on the lab bench and a hot plate, respectively.

Each peel experiment was conducted in several steps. First, TPM tape, cut to 30 mm by 220 mm, was attached to the substrate with a uniform pressure of 0.15 Pa applied for 10 s at 25 °C. Next, the substrate was brought to the desired temperature through one of the methods described previously and dwelled for 600s. Finally, the peel test was performed with a peel rate of 1 mm/s over a total peel length of 160 mm (TA.XTplusC Texture Analyser, Stable Micro Systems). The average peel force was determined for the peel region from 40 mm to 120 mm. All results are reported as peel force since the sample geometry was held constant.

3. Results and Discussion

3.1 Dynamic shear moduli of PSAs

[Figure 3 near here]

The performance of a PSA is highly dependent on its bulk viscoelastic properties, which generally control the conformability and adhesive strength. To increase contact area on a rough surface and form a strong bond, a PSA must remain in the rubbery plateau zone over the range of operating temperatures.[20] Therefore, it is important that the typical operating temperature window lie within the PSA's rubbery plateau zone. Figure 3 shows the viscoelastic behavior, highlighting the onset temperature of the rubbery plateau zones of PSAs of each TPM tape over the temperature range of interest. The blue dotted line indicates the transition temperature (T_R) from the glass transition zone (shaded) to the rubbery plateau zone (unshaded), which is defined as the temperature at which $tan\,\delta = 1$.[23] All the tapes tested here have a T_R within the range of investigated temperatures as shown in Figure 3. The shear storage moduli (G') and loss moduli (G") of the PSAs were constant or slightly decreased with increasing temperature and showed greater elastic behavior than viscous behavior above T_R. Below T_R, all tapes showed noisy, random results since the storage and loss moduli of the PSAs exceeded the capacity of the DMA load cell. Based on the results, optimal operating temperatures of all TPM tapes were defined. In the tested temperature range, Tape C has the widest operating temperature range, from -15 °C to 40 °C and tapes D shows the smallest operating temperature range, from 5 °C to 40 °C. The operating temperature ranges of Tape A and B are from -7 °C to 40 °C and 0 °C to 40 °C, respectively.

3.2 Dynamic mechanical properties of the top layer

[Figure 4 near here]

The dynamic mechanical properties of the top layer were measured over the same temperature range used for the PSAs and are shown in Figure 4. Here, the dashed line indicates

the glass transition temperature (T_g) of the top layer, defined as the peak of $tan\ \delta$.[24] Below T_g, the storage modulus of the top layer dramatically increased. Tapes A and B had glass transition temperatures near -5 °C, and the glass transition temperature of Tape C was near 0 °C as shown in Figure 4. The glass transition temperature of Tape D was not in the performing temperature, but likely falls below -20 °C.

3.3 Peel test of TPM tapes

[Figure 5 near here]

A 90° peel test was performed utilizing a custom-built fixture[22] on a stainless-steel surface on each tape at various surface temperatures (-20 °C, 0 °C, 25 °C, and 40 °C) as shown in Figure 2 (b). A stainless-steel box was used to set and maintain each temperature. The temperature was maintained within ± 3 °C of the set temperature during the 120s pre-test, dwell and test. Figure 5(a) shows the peel responses of TPM tapes at the tested temperatures. Except for the profiles at -20 °C, the peel responses for all types of TPM tape have small fluctuations. Because each tape has a different size and distribution of ridges for Tape A and C and glass beads for Tape B and D as shown in Figure 1(b), the magnitudes of these fluctuations varied. Adhesive failure was observed in all TPM tapes at the tested temperatures. A brittle broken fracture mode was observed at -20 °C for Tapes A and B as shown in Figure 5 (a and b). In this mode, the peel force increased significantly and then rapidly decreased to close to 0N in a cyclic manner over the course of the peel test.

[Figure 6 near here]

The average peel force was calculated over the peeling length from 40 mm to 120 mm for each test. These individual average peel force values were subsequently averaged for each tape and substrate temperature (Figure 6). The dotted and dashed lines indicate the T_R of the PSAs and

T_g of the top layer, respectively. The peel force of Tapes A and B increased as the temperature decreased to 0 °C, and decreased at -20 °C. The peel forces of Tapes C and D decreased inversely with temperature as shown in Figure 6 (c and d). Generally, the adhesive peel force is dependent on geometric and mechanical conditions such as adhesive thickness, peel velocity, and the modulus and thickness of the top layer.[9,25] Therefore, it can be complicated to compare the peel force for each TPM tape. However, the peel force with respect to the substrate temperature can be explained through viscoelastic relationships for each tape. The plateau modulus and loss tangent of the PSAs are inversely proportional to temperature as shown in Figure 3. Jensen et al.[18] defined an empirical relationship between viscoelastic parameters such as plateau modulus (G_0), loss tangent ($tan\ \delta$), and PSA peel force (P_{peel}), as in Equation 1.

$$\frac{P_{peel}}{tWG_0} \propto f\left(tan\delta_{\omega_{peel}}\right) \quad (1)$$

where t is the thickness, w is the width, and ω_{peel} is the peel frequency defined as the inverse of peel velocity. It is important to note that the loss tangent is a function ($f\left(tan\delta_{\omega_{peel}}\right)$) since peel force is not directly proportional to but dependent on the loss tangent. Equation 1 explains the observation that the peel force for each TPM tape decreased as temperature increased. Energy dissipation increased as the loss tangent increased, so the peel force also increased.

[Figure 7 near here]

The brittle broken fracture mode was observed at -20 °C for tapes in which both the T_g of the top layer and T_R of the PSA are above -20 °C. As a result, the average peel force decreased at -20 °C for tapes A and B. Below T_g, the bending stiffness of the top layer increases dramatically. Below T_R, the PSA becomes harder to deform and loses conformability, which decreases the adhesive strength by preventing full contact with the surface. As a result, it is expected that bending

strength of the top layer and the adhesive strength of PSAs compete during the peel test, resulting in the distinctive sawtooth shape of the peel force with distance plot (Figure 5 (a and b)).

Figure 7 (a and b) explains this brittle broken fracture behavior in the context of TPM tapes - here, the tape spontaneously peels off (positions from 0 to x_1) at less than a 90° peel angle. The peel force then increased with the peel angle from θ_1 to θ_2, but there was no peeling. This behavior repeated over the peel test and is represented in the peel profile in Figure 5 (a, b) at -20 °C. Since the bending stiffness of the top layer is greater than the interface strength between PSAs and the surface, the tape peeled before the local angle between tape and surface reached 90°. The video for brittle broken fracture, which was taken during 90° peel test for Tape B at -20 °C, is provided in the supplemental material.

Although both T_g and T_R for Tape C were higher than -20 °C, the brittle broken fracture mode was not observed. This is likely because of the structure of the top layer. Raised ridges are distributed across the top layer surface as shown in Figure 1 (b, iii). Each ridge region is thicker and therefore stiffer than the flat regions in between.[26] Brittle broken fracture occurred only in the ridge region as shown in Figure 5 (c). The peel lengths of the peak and valley regions in the peel profile correspond well with the distance between ridges (flat region) and the length of the ridge as shown in Figure 5 (c) and Figure 1 (b, iii).

Based on the peel behavior at various temperatures of the substrate, the usable temperature range can be determined for each TPM tape. During construction at very cold temperatures, Tapes C and D would be expected to have better adhesive performance than Tapes A or B. On the other hand, Tapes B and D would be expected to have better adhesive performance under high-

temperature construction conditions since the peel force of these tapes is higher than the others at elevated temperatures.

4. Conclusion

Viscoelastic and mechanical properties directly influence the adhesion strength for TPM tapes. It is critical to characterize these properties at at operating temperatures expected during road construction. However, measuring the viscoelastic properties of only the PSA in TPM tapes is limited with conventional rheological configurations. Here, a double lap shear fixture was created to measure the dynamic mechanical properties for the PSA in TPM tapes, and an operating temperature window for four brands of TPM tapes was determined empirically. While considering the viscoelastic properties of the PSAs and top layers, the interfacial failure modes and peel forces were analyzed over the expected operating temperature range. All tested TPM tapes failed adhesively at temperatures above the T_g of the top layer and the T_R of the PSAs. The peel force decreased as temperature increased due to a reduction in storage modulus. At -20 °C, the temperature was below T_g of the top layer and T_R of the PSA for Tapes A and B – here, the brittle broken fracture mode was observed. This was due to a combination of the increased bending stiffness of the top layer and the decreased adhesion of PSA in the 90° peel test. Using this method, the potential operating temperatures of commercial TPM tapes can be determined, which could inform future TPM product evaluation and selection. Further, by considering the required operating temperature range for these products, new and improved TPM tapes can be developed.

Acknowledgements

This work was supported by the Joint Transportation Research Program administered by the Indiana Department of Transportation and Purdue University under Project Number SPR-4423. The authors would like to thank 3M, Brite Line, Swarco, and ATM for providing tape materials.

Special thanks to Dawson Smith for helpful discussions.

Declaration of Interest

The authors declare no conflicts of interest.

Word Count: 4432

References

[1] E. T. Donnell, G. R. Chehab, X. Tang, D. Schall, Exploratory analysis of accelerated wear testing to evaluate performance of pavement markings.*Transp. Res. Rec. J. Transp. Res. Board.* **2009**, *2107*, 76–84. DOI: 10.3141/2107-08.

[2] J. T. Lee, T. L. Maleck, W. C. Taylor, Pavement marking material evaluation study in Michigan.*Inst. Transp. Eng.* **1999**, *69*, 44–51.

[3] N. Hawkins, O. Smadi, B. Aldemir-Bektas, Smart Work Zone Deployment Initiative: Evaluating the Effectiveness of Temporary Work-Zone Pavement Marking Products.*Cent. Transp. Res. Educ. Iowa State Univ. Ames, IA, US* **2012**.

[4] Y. Cho, J.-H. Pyeon, K. Kabassi, J.-H. Pyeon, K. Choi, C. Wang, T. Norton, Effectiveness Study of Methods for Removing Temporary Pavement Markings in Roadway Construction Zones.*J. Constr. Eng. Manag.* **2013**, *139*, 257–266. DOI: 10.1061/(asce)co.1943-7862.0000608.

[5] B. E. Gdalin, E. V. Bermesheva, G. A. Shandryuk, M. M. Feldstein, Effect of temperature on probe tack adhesion: Extension of the dahlquist criterion of tack.*J. Adhes.* **2011**, *87*, 111–138. DOI: 10.1080/00218464.2011.545325.

[6] S. gun Chu, Dynamic mechanical properties of pressure sensitive adheisive.*1st* Ed.: L.-H. Lee, Springer, Boston, MA, **1991**, pp. 97–138.

[7] J. M. L. Dos Reis, Effect of temperature on the mechanical properties of polymer mortars.*Mater. Res.* **2012**, *15*, 645–649. DOI: 10.1590/S1516-14392012005000091.

[8] J.J. Aklonis, Mechanical properties of polymers.*J. Chem. Educ.* **1981**, *58*, 892–897. DOI: 10.1201/ed058p892.

[9] C. Creton, Pressure-sensitive adhesives: An introductory course.*MRS Bull.* **2003**, *28*, 434–

439. DOI: 10.1557/mrs2003.124.

[10] H. K. Chan, G. J. Howard, Structure-Property Relationships in Acrylic Adhesives.*J. Adhes.* **1978**, *9*, 279–304. DOI: 10.1080/00218467808075121.

[11] D. H. Kaelble, Peel Adhesion: Influence of Surface Energies and Adhesive Rheology.*J. Adhes.* **1969**, *1*, 102–123. DOI: 10.1080/00218466908078882.

[12] J. B. Class, S. G. Chu, The viscoelastic properties of rubber–resin blends. II. The effect of resin molecular weight.*J. Appl. Polym. Sci.* **1985**, *30*, 815–824. DOI: 10.1002/app.1985.070300230.

[13] A. Zosel, Adhesion and tack of polymers: Influence of mechanical properties and surface tensions.*Colloid Polym. Sci.* **1985**, *263*, 541–553. DOI: 10.1007/BF01421887.

[14] F. Saulnier, T. Ondarçuhu, A. Aradian, E. Raphaël, Adhesion between a viscoelastic material and a solid surface.*Macromolecules* **2004**, *37*, 1067–1075. DOI: 10.1021/ma021759t.

[15] E. P. Chang, Viscoelastic properties of pressure-sensitive adhesives.*J. Adhes.* **1997**, *60*, 233–248. DOI: 10.1080/00218469708014421.

[16] S. Sun, M. Li, A. Liu, A review on mechanical properties of pressure sensitive adhesives.*Int. J. Adhes. Adhes.* **2013**, *41*, 98–106. DOI: 10.1016/j.ijadhadh.2012.10.011.

[17] G. I. Ozturk, A. J. Pasquale, T. E. Long, Melt synthesis and characterization of aliphatic low-Tg polyesters as pressure sensitive adhesives.*J. Adhes.* **2010**, *86*, 395–408. DOI: 10.1080/00218460903418303.

[18] M. K. Jensen, A. Bach, O. Hassager, A. L. Skov, Linear rheology of cross-linked polypropylene oxide as a pressure sensitive adhesive.*Int. J. Adhes. Adhes.* **2009**, *29*, 687–693. DOI: 10.1016/j.ijadhadh.2008.10.005.

[19] C. A. Dhlquist, Pressure-sensitive adhesive.Ed.: R.L. Patrick, New York, M. Dekker, **1969**, p. 219.

[20] D. H. Lim, H. S. Do, H. J. Kim, PSA performances and viscoelastic properties of SIS-based PSA blends with H-DCPD tackifiers.*J. Appl. Polym. Sci.* **2006**, *102*, 2839–2846. DOI: 10.1002/app.24571.

[21] F. X. Gibert, A. Allal, G. Marin, C. Derail, Effect of the rheological properties of industrial hot-melt and pressure-sensitive adhesives on the peel behavior.*J. Adhes. Sci. Technol.* **1999**, *13*, 1029–1044. DOI: 10.1163/156856199X00497.

[22] J. A. Gohl, T. C. Thiele-Sardina, M. L. Rencheck, K. A. Erk, C. S. Davis, A Modular Peel Fixture for Tape Peel Tests on Immovable Substrates.*Exp. Mech. [Online early access]* **2021**, DOI 10.1007/s11340-021-00738-1.

[23] I. Benedek, M. M. Feldstein, Handbook of Pressure-Sensitive Adhesives and Products.*Handbook of Pressure-Sensitive Adhesives and Products*, CRC Press, Boca Raton, FL, **2008**.

[24] J. Michels, R. Widmann, C. Czaderski, R. Allahvirdizadeh, M. Motavalli, Glass transition evaluation of commercially available epoxy resins used for civil engineering applications.*Compos. Part B Eng.* **2015**, *77*, 484–493. DOI: 10.1016/j.compositesb.2015.03.053.

[25] M. Zhou, N. Pesika, H. Zeng, J. Wan, X. Zhang, Y. Meng, S. Wen, Y. Tian, Design of gecko-inspired fibrillar surfaces with strong attachment and easy-removal properties: A numerical analysis of peel-zone.*J. R. Soc. Interface* **2012**, *9*, 2424–2436. DOI: 10.1098/rsif.2012.0200.

[26] M. L. Rencheck, J. A. Gohl, H. P. Grennan, K. A. Erk, C. S. Davis, Assessing the Elastic

Moduli of Pavement Marking Tapes using the Tape Drape Test.*Transp. Res. Rec. J. Transp. Res. Board [Online early access]* **2021**, 1–10. DOI: 10.1177/0361198121999623.

Table 1. Thickness of the top layer and PSA layer for TPM tapes.

	Tape A	**Tape B**	**Tape C**	**Tape D**
Top Layer (μm)	775 ± 26	755 ± 87	482 ± 49	568 ± 18
PSA (μm)	275 ± 27	158 ± 24	139± 15	464 ± 31

Figure 1.

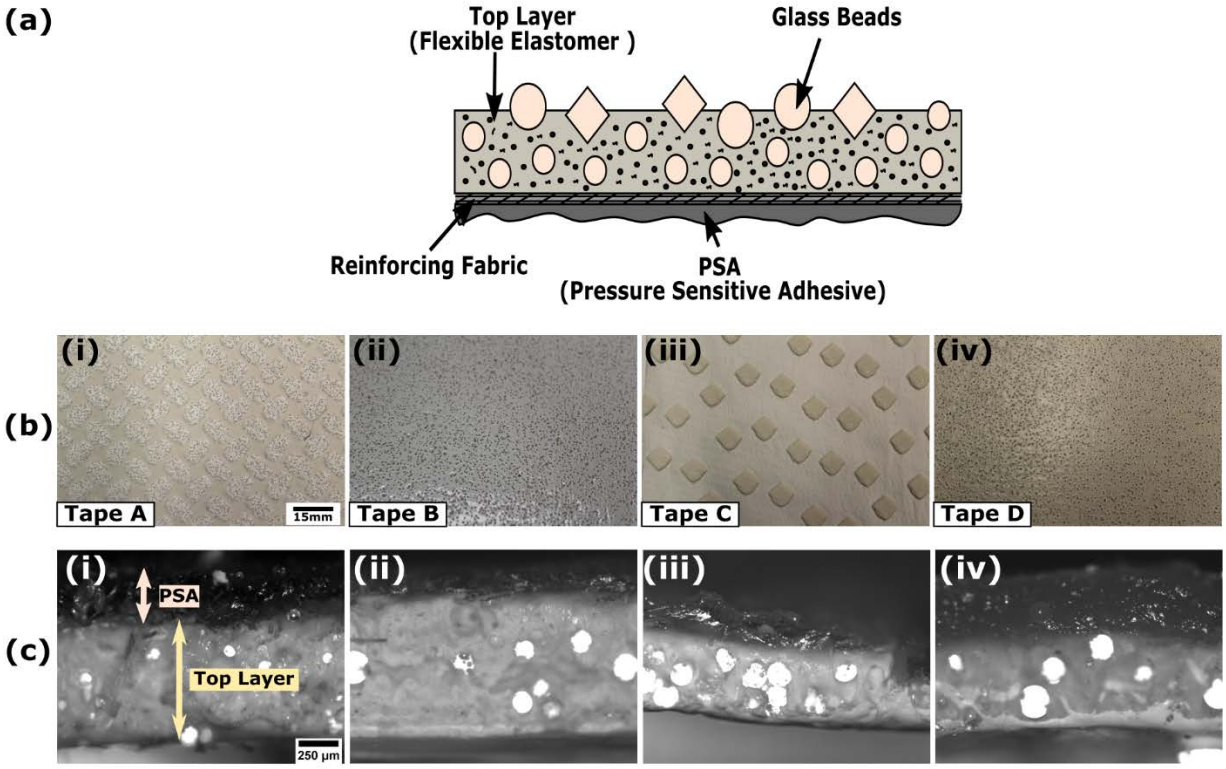
(a)
Top Layer
(Flexible Elastomer)
Glass Beads
Reinforcing Fabric
PSA
(Pressure Sensitive Adhesive)
(b)
(i)
(ii)
(iii)
(iv)
Tape A
15mm
Tape B
Tape C
Tape D
(c)
(i)
PSA
Top Layer
250 µm
(ii)
(iii)
(iv)

Figure 2

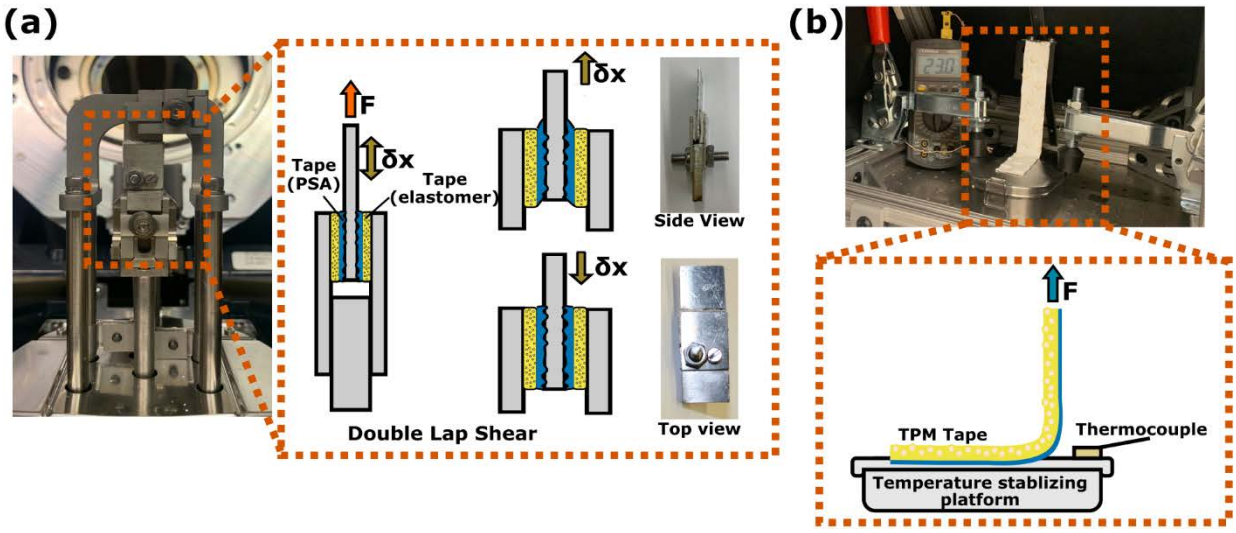
(a)
F
δx
Tape
(PSA)
Tape
(elastomer)
δx
Side View
δx
Top view
Double Lap Shear
(b)
F
TPM Tape
Thermocouple
Temperature stablizing
platform

Figure 3

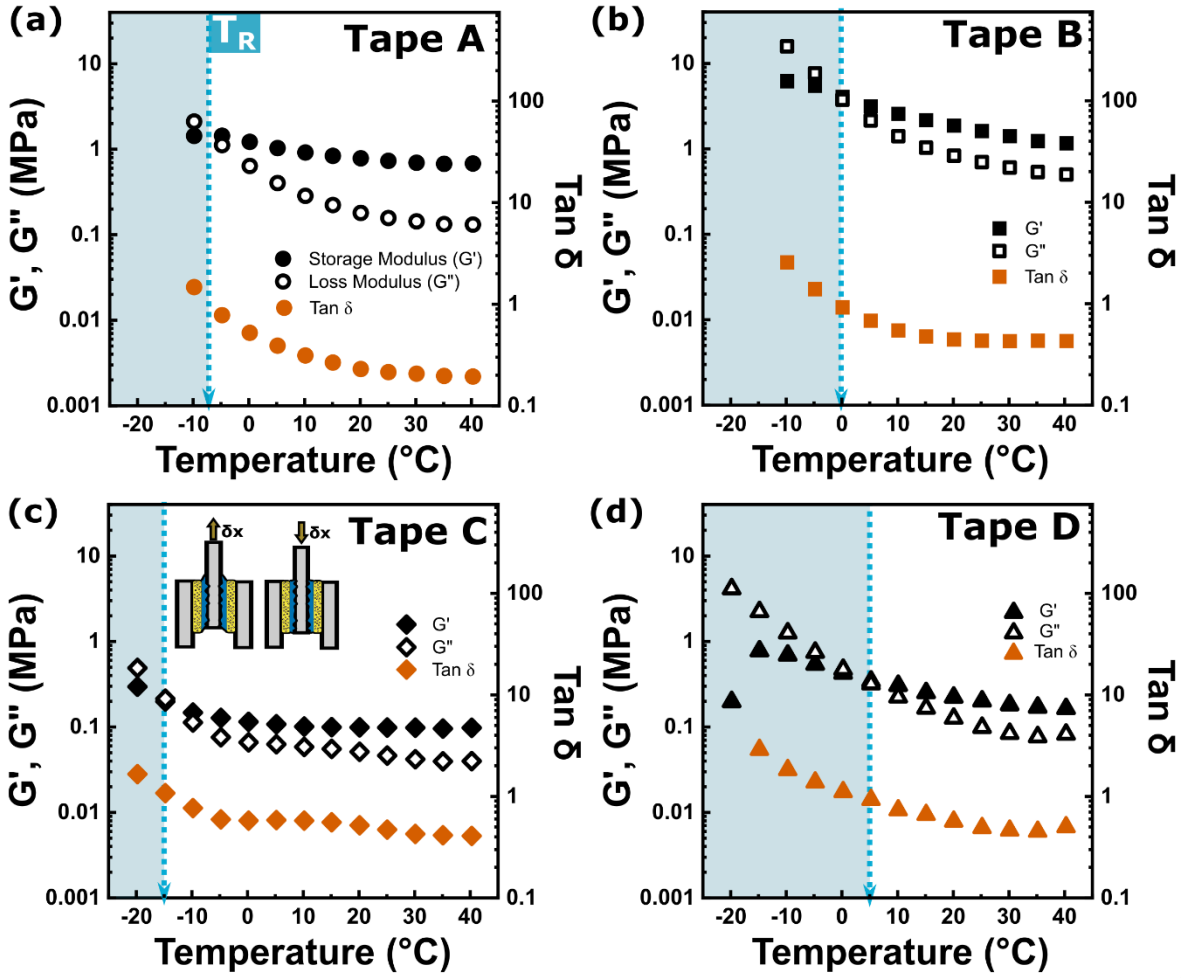
(a)
Tape A
T_R
Storage Modulus (G')
Loss Modulus (G")
Tan δ
G', G" (MPa)
Tan δ
Temperature (°C)
(b)
Tape B
G'
G"
Tan δ
(c)
Tape C
δx
δx
(d)
Tape D

Figure 4.

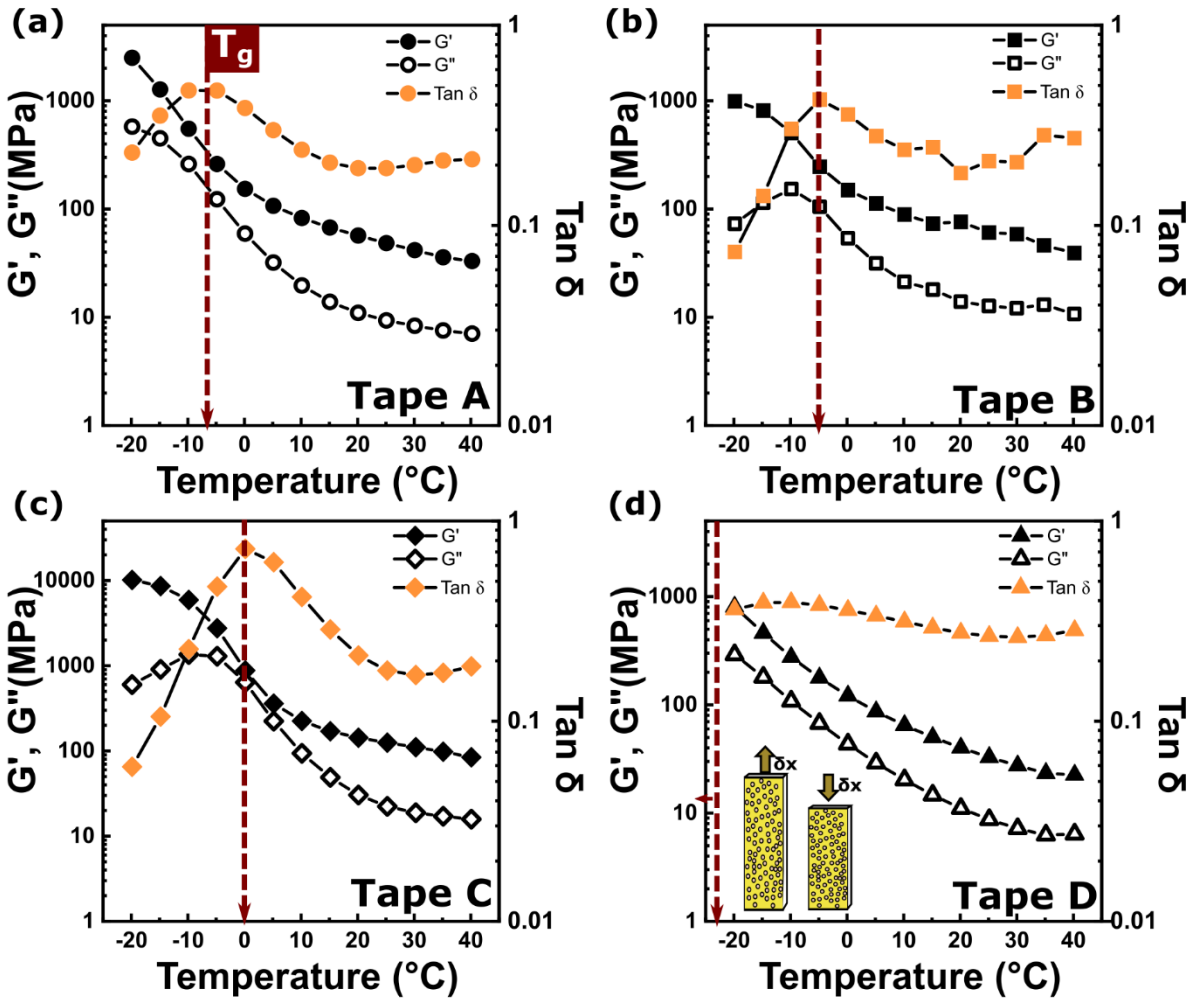
(a)
Tg
G'
G"
Tan δ
Tape A
G', G"(MPa)
Tan δ
Temperature (°C)
(b)
Tape B
(c)
Tape C
(d)
Tape D
δx
δx

Figure 5

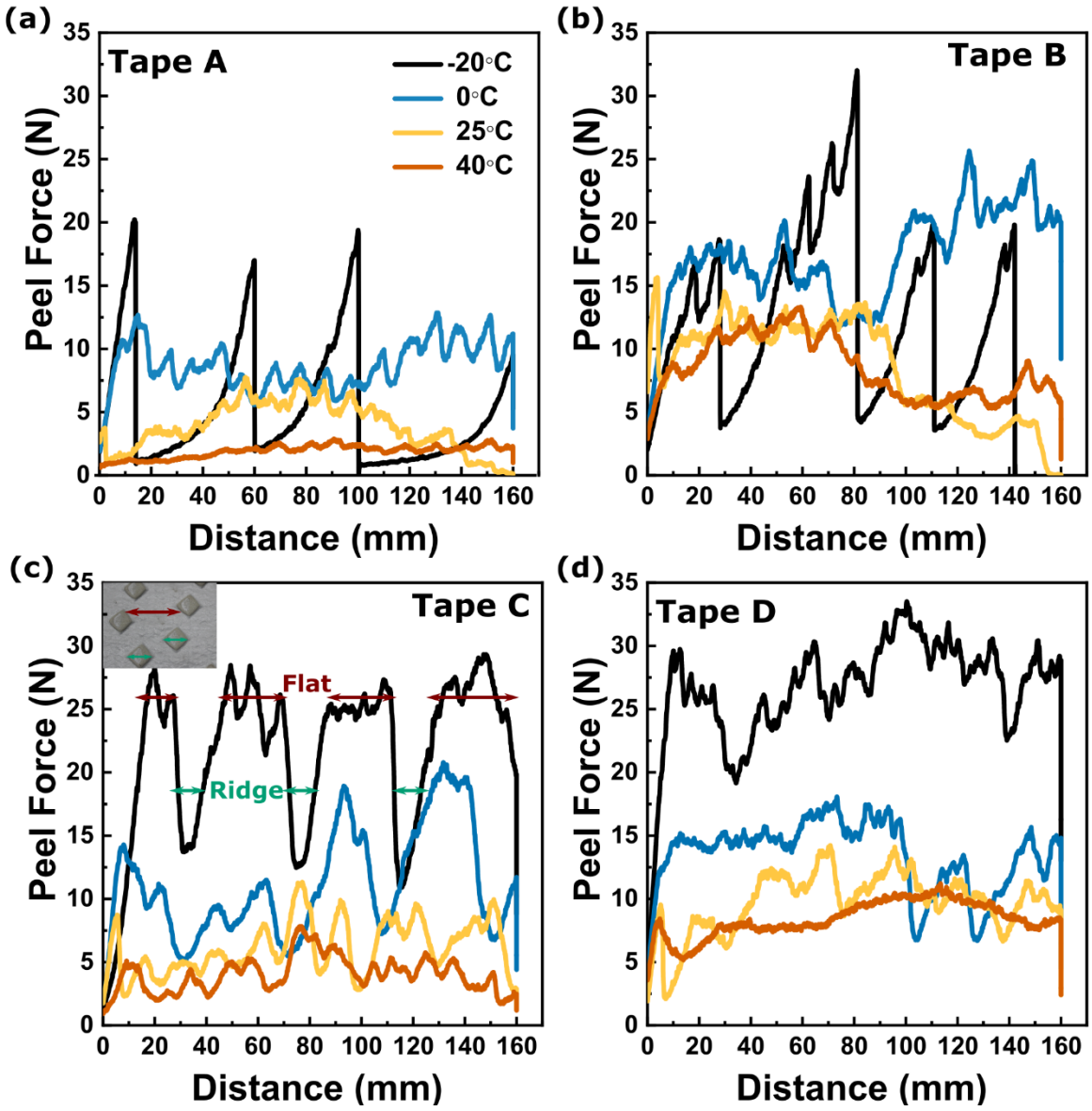
(a)
Tape A
-20°C
0°C
25°C
40°C
Peel Force (N)
Distance (mm)
(b)
Tape B
Peel Force (N)
Distance (mm)
(c)
Tape C
Flat
Ridge
Peel Force (N)
Distance (mm)
(d)
Tape D
Peel Force (N)
Distance (mm)

Figure 6

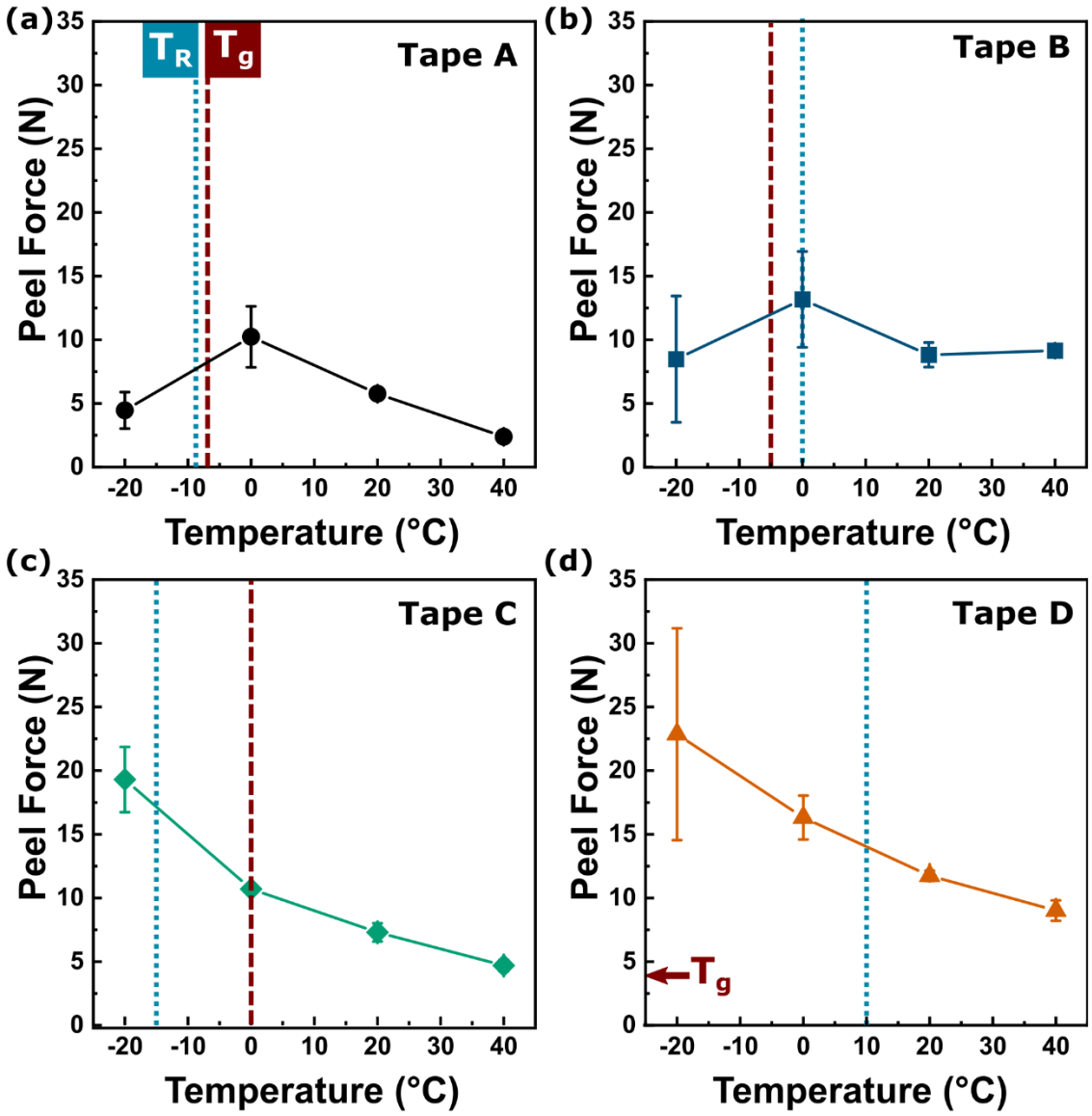
(a)
Tape A
T_R
T_g
Peel Force (N)
Temperature (°C)
(b)
Tape B
Peel Force (N)
Temperature (°C)
(c)
Tape C
Peel Force (N)
Temperature (°C)
(d)
Tape D
T_g
Peel Force (N)
Temperature (°C)

Figure 7

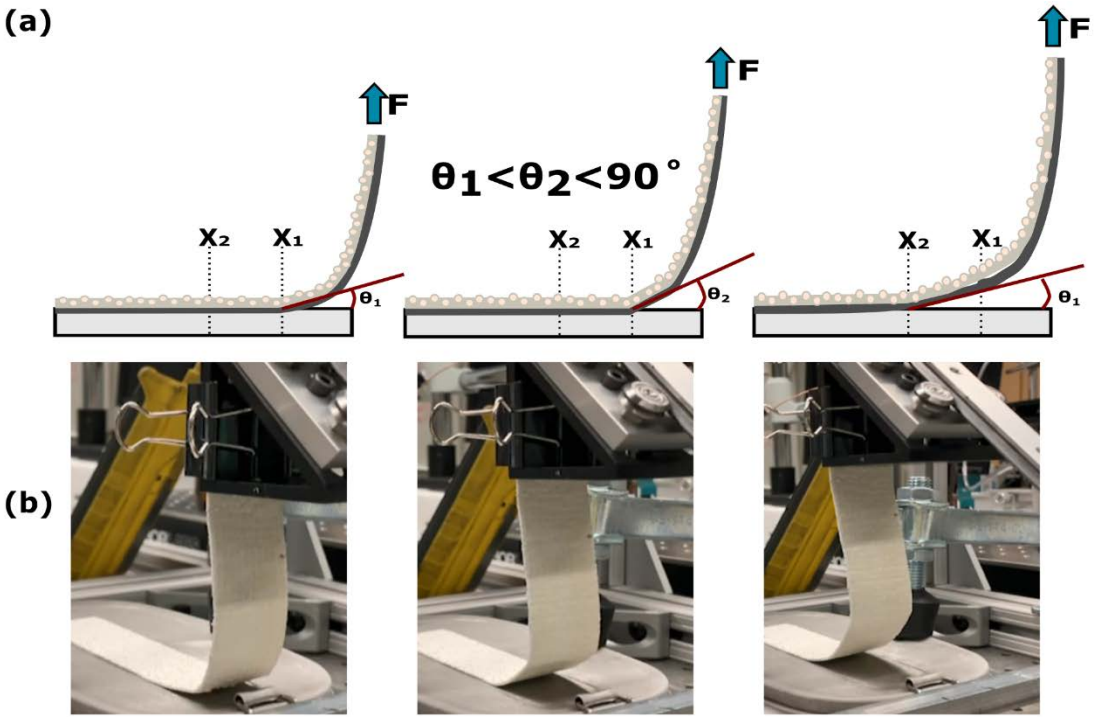

Figure 1. (a) schematic image of typical structure for TPM tapes. (b) Top views of (i) Tape A, (ii) Tape B, (iii) Tape C, and (iv) Tape D. (c) Microscopic side view images of (i) Tape A, (ii) Tape B, (iii) Tape C, and (iv) Tape D.

Figure 2. (a) Double lap shear fixture. The left image shows the double lap shear fixture clamped on the DMA instrument. The right schematic image shows the side view of the double lap shear fixture with TPM tape. Inserted images are the top and side views of the fixture. (b) Photograph of 90° peel test fixture and schematic of peel test configuration with TPM tapes.

Figure 3. The dynamic mechanical behavior of PSAs for (a) Tape A, (b) Tape B, (c) Tape C, and (d) Tape D. The vertical dotted line on each plot indicates the transition temperature (T_R) from transition zone (shaded region) to rubbery plateau zone. Inserted schematic image in (c) shows double lap shear configuration for PSA. A 0.5% oscillatory shear strain was applied to the PSAs at a frequency of 1 Hz. The temperature was increased from -20 °C to 40 °C in 5 °C increments with dwell time for 120s at each temperature.

Figure 4. The dynamic mechanical behavior of top layers for (a) Tape A, (b) Tape B, (c) Tape C, and (d) Tape D. The vertical dashed line indicates the glass transition temperature (T_g) of the top layer. Inserted schematic image in (d) shows the tensile configuration for top layer. A 0.2% oscillatory tensile strain was applied to the top layer at a frequency of 1Hz. The temperature was increased from -20 °C to 40 °C in 5 °C increments with dwell time for 120s at each temperature.

Figure 5. The 90° peel force with a distance of (a) Tape A, (b) Tape B, (c) Tape C, and Tape D at various temperatures. The inset image in (c) exhibits the top view of Tape C and red and blue arrows indicate the flat and ridge position, respectively. The peel test was performed with 1mm/s peel rate.

Figure 6. The average peel force with respect to the temperature for (a) Tape A, (b) Tape B, (c) Tape C, and (d) Tape D. The dotted and dashed lines show transition temperature from transition zone to rubbery plateau zone of PSAs and glass transition temperature of the top layers, respectively. The error bars represent one standard deviation over 3 tests.

Figure 7. (a) Schematic and (b) photographic image sequence illustrating the brittle broken fracture phenomenon shown in Figure 6 (a) and (b) at -20 °C. (b) The image was taken on the peel test for Tape B at -20 °C.